Two-Dimensional Numerical Simulation of AlGaN/GaN HEMTs

S. Vitanov[1], V. Palankovski[1], R. Quay[2], and E. Langer[1]

[1] TU Vienna, Inst. for Microelectronics, Gußhausstraße 27–29, 1040 Vienna, Austria
Email: {vitanov,palankovski,langer}@iue.tuwien.ac.at
[2]Fraunhofer Inst. for Solid-State Physics (IAF), Tullastraße 72, 79108 Freiburg, Germany
Email: ruediger.quay@iaf.fraunhofer.de

***Abstract*— The GaN material system is modeled and introduced in the two-dimensional device simulation tool Minimos-NT. The simulation setup is calibrated against measurement data from AlGaN/GaN HEMTs. Further, the impact of gate field plates on the electric field distribution in the channel for different geometry setups is investigated.**

I. Introduction

The rapid evolution of the telecommunications technologies in the last decade has posed a new challenge to the microelectronics industry. RF sources and power amplifiers are required in base station transmitters for cellular telephone systems, satellite transmitters, high-definition television (HDTV) transmitters, power modules for phased-array radars, surveillance and traffic control radars. Development of a solid-state solution for these applications has turned out to be one of the last frontiers for semiconductor electronics. Such a solution must include attributes of ultra-high power combined with high efficiency, linearity, and manufacturability. Even though the importance of these features are specified by the application, only a few technologies can satisfy the majority of the needs simultaneously. One is the GaN-based family of semiconductors. Historically the material was one of the first III-V compound semiconductors to be studied [1]. The interest declined in the early 1980s as continuous problems achieving p-type doping could not be overcome. The breakthrough came in the late 1980s when the first films on sapphire substrates were realized [2] and later in the 1990s when a post-growth thermal treatment was introduced [3]. Only one year later the first AlGaN/GaN high electron mobility transistors (HEMTs) were demonstrated [4]. Since then GaN HEMTs are an object of ongoing research interest. Starting at a cut-off frequency f_T=11 GHz [5], values of f_T=163 GHz were reached recently [6]. RF power applications also require devices with high breakdown voltage (V_{BR}). Due to its wide bandgap GaN features a high critical electric field of breakdown. Further enhancements can be achieved by adopting a field plate technique [7]. With its origins in the context of high voltage p-n junctions [8] the field plate reduces the peak electric field values in the channel. This allows breakdown voltages as high as 1900 V, while a low R_{on} of $\sim$2.2 mΩ cm^2 is maintained [9]. Material attributes, such as the high peak and saturation velocity and high electron mobility are also the reason for the excellent microwave performance.

Thus, AlGaN/GaN HEMTs have established themselves as microwave power devices. However, they are still designed primarily with experimental empirical techniques. Simulation software is used to improve individual device characteristics after calibration of the simulation model parameters. For such purpose a fast simulation turnaround is typically preferred, at the expense of the physical depth of the models employed. The latter can lead to a restrictive design space. Therefore, a reasonable tradeoff between model complexity and computational time must be found.

II. The Device Simulation Tool

In this work we use the in-house developed simulator Minimos-NT [10]. It is a general-purpose semiconductor device simulation tool which features the capability to consider various semiconductor materials, and also complex geometry structures. The box integration method is used to discretize the conservation equations [11]. The basic equations solved in a device simulator are the Poisson equation and the current continuity equations for electrons and holes (1)-(3). The unknown quantities are the electrostatic potential ψ and the electron and hole concentration n and p. C denotes the net concentration of the ionized dopants, ε is the dielectric permittivity of the semiconductor, and R is the net recombination rate. E_C and E_V are the position-dependant band energies, $N_{C,0}$ and $N_{V,0}$ the effective density of states.

Since the longitudinal electric field in the device channel reaches very high values of above 500 kV/cm, a hydrodynamic approach must be used in order to properly model the carrier transport and energy relaxation. It allows the carrier temperature to be different from the lattice temperature. The basic equations are completed through two additional equations describing the conservation of the average carrier energies, (4) and (5). T_n and T_p denote the carrier temperatures, $\tau_{w,n}$ and $\tau_{w,p}$ are the energy relaxation times, S_n and S_p the energy fluxes. Self-heating effects are accounted for by solving the lattice heat flow equation (6) self-consistently.

Since HEMTs are unipolar devices, in the particular examples presented in this work, the equations for holes, (3) and (5), are neglected. A global lattice temperature model [12] is used for further reduction of complexity, which is solved together with a system of three partial differential equations (1), (2), and (4).

The complex device geometry is partitioned into independent logical units, so-called segments, which consist of diverse materials. Different models and algorithms are applied in the segments, e.g. the hydrodynamic transport model is used in the channel and the drift-diffusion transport model in all other segments. The segments are linked together through interface models, which account for the interface conditions, depending on the type of the junction.

$$\mathrm{div}\,(\varepsilon \cdot \mathrm{grad}\ \psi) = \mathrm{q} \cdot (n - p - C) \tag{1}$$

$$\mathrm{div}\left(\mu_n \cdot n \cdot \left(\mathrm{grad}\left(\frac{E_C}{\mathrm{q}} - \psi\right) + \frac{\mathrm{k_B}}{\mathrm{q}} \cdot \frac{N_{C,0}}{n} \cdot \mathrm{grad}\left(\frac{n \cdot T_n}{N_{C,0}}\right)\right)\right) = R + \frac{\partial n}{\partial t} \tag{2}$$

$$\mathrm{div}\left(\mu_p \cdot p \cdot \left(\mathrm{grad}\left(\frac{E_V}{\mathrm{q}} - \psi\right) - \frac{\mathrm{k_B}}{\mathrm{q}} \cdot \frac{N_{V,0}}{p} \cdot \mathrm{grad}\left(\frac{p \cdot T_p}{N_{V,0}}\right)\right)\right) = -R - \frac{\partial p}{\partial t} \tag{3}$$

$$\mathrm{div}\ \mathbf{S}_n = \mathrm{grad}\left(\frac{E_C}{\mathrm{q}} - \psi\right) \cdot \mathbf{J}_n - \frac{3 \cdot \mathrm{k_B}}{2} \cdot \left(\frac{\partial\,(n \cdot T_n)}{\partial t} + R \cdot T_n + n \cdot \frac{T_n - T_\mathrm{L}}{\tau_{w,n}}\right) \tag{4}$$

$$\mathrm{div}\ \mathbf{S}_p = \mathrm{grad}\left(\frac{E_V}{\mathrm{q}} - \psi\right) \cdot \mathbf{J}_p - \frac{3 \cdot \mathrm{k_B}}{2} \cdot \left(\frac{\partial\,(p \cdot T_p)}{\partial t} + R \cdot T_p + p \cdot \frac{T_p - T_\mathrm{L}}{\tau_{w,p}}\right) \tag{5}$$

$$\mathrm{div}(\kappa_\mathrm{L} \cdot \mathrm{grad}\ T_\mathrm{L}) = \rho_\mathrm{L} \cdot c_\mathrm{L} \cdot \frac{\partial T_\mathrm{L}}{\partial t} + H \tag{6}$$

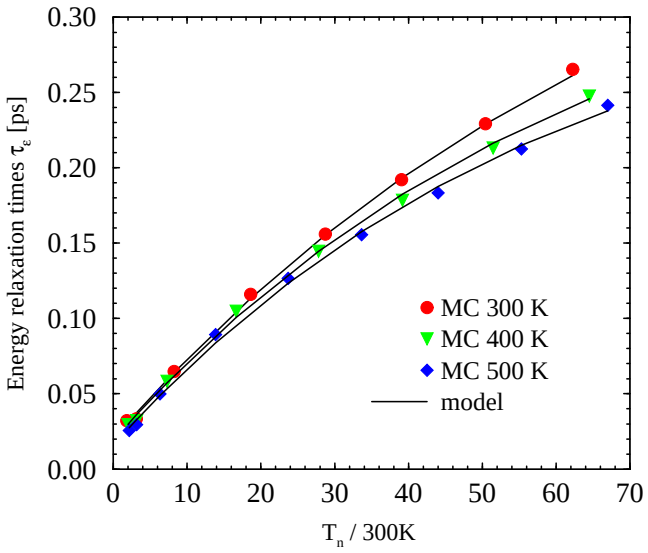

Fig. 1. Electron energy relaxation times in GaN as a function of electron temperature for different lattice temperatures. Comparison between model and MC simulation data.

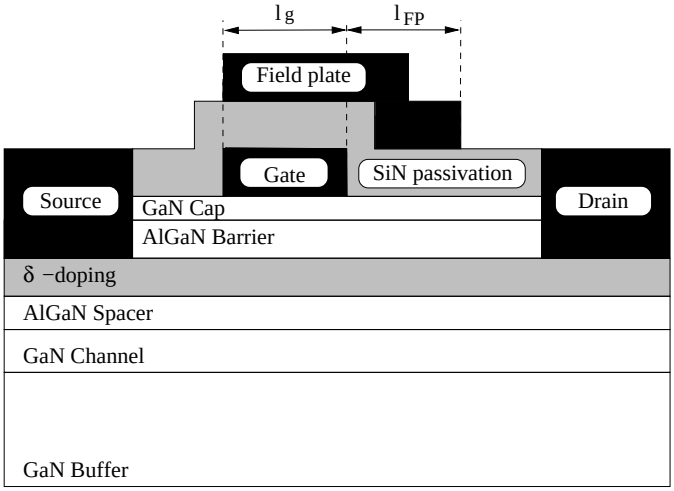

Fig. 2. A schematic layer structure of a single heterojunction AlGaN/GaN HEMT device with field plate.

For all materials Minimos-NT employs universal models with different parameter sets. Therefore, a proper material parameter set is of great importance for the quality of the device simulation. We have conducted an extensive literature research to gain such a parameter set. The data we use for our device simulations have been verified against measurement results and own Monte Carlo (MC) simulation data in [13]. As an example, Fig. 1 shows the electron energy relaxation time ($\tau_{w,n}$) in GaN as a function of the electron temperature for different lattice temperatures. The symbols represent data obtained by Monte Carlo simulation, the curves are the analytical models implemented in Minimos-NT.

III. Calibration

Our simulator is calibrated against measurement data from devices produced at IAF (Freiburg). The AlGaN/GaN HEMT technology is based on multi-wafer MOCVD growth on 2-inch semi-insulating SiC substrates based on an Aixtron 2000 multi-wafer reactor. The gate technology is so far e-beam defined with a gate length of l_g =150 nm, 300 nm, and 600 nm. Device isolation is achieved by mesa isolation. Fig. 2 gives an example of a typical fully planar AlGaN/GaN HEMT field-plated structure. An $\mathrm{Al_xGa_{x-1}N}$/GaN heterointerface is grown on top of a thick insulating GaN buffer. The material composition amounts to x=0.3. All layers are not intentionally doped (nid), except the δ-doping which is introduced in the AlGaN supply layer to provide additional carriers and to improve the access resistance. A gate Schottky contact controls the carrier flow in the channel.

The crucial factor building the channel in HEMTs are the polarization charges at the AlGaN/GaN heterointerfaces. The positive charge at the channel/spacer interface is compensated by a negative surface charge at the barrier/ cap interface. The optimum value of 1.1×10^{13} $\mathrm{cm^{-2}}$ is found (Fig. 3). As can be seen in Fig. 4 (the electron concentration for V_DS=7 V, V_GS=0 V is shown) the device is a normally on transistor. Another unknown is the penetration depth of the drain/source metal contacts which may build an alloy with the AlGaN supply layer. We assume a metal diffusion to the δ-doping in our simulations. We further assess the impact of thermionic emission and field emission (tunneling) effects which critically determine the current transport across the heterojunctions. An optimal tunnel length of 7.5 nm is found.

Fig. 5 shows simulated (lines) and measured (symbols) data for the transfer curves with and without field plate. In Fig. 6 the measured and simulated output characteristics are compared. As can be seen a good agreement has been achieved for both devices.

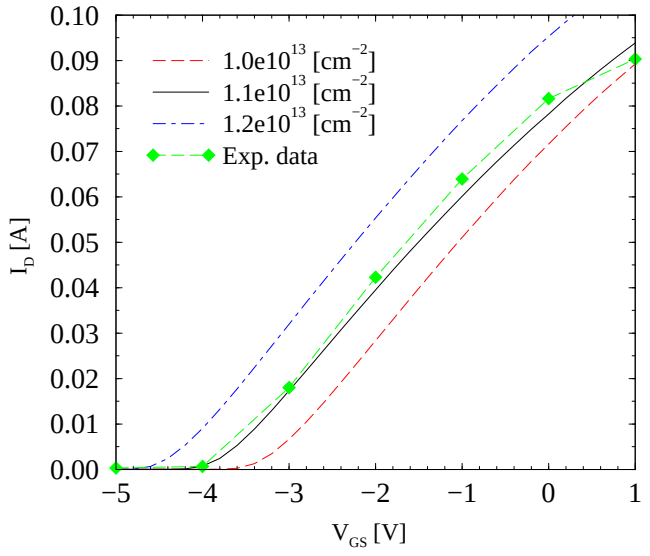

Fig. 3. Transfer characteristics for different polarization charge densities at the AlGaN/GaN heterojunctions.

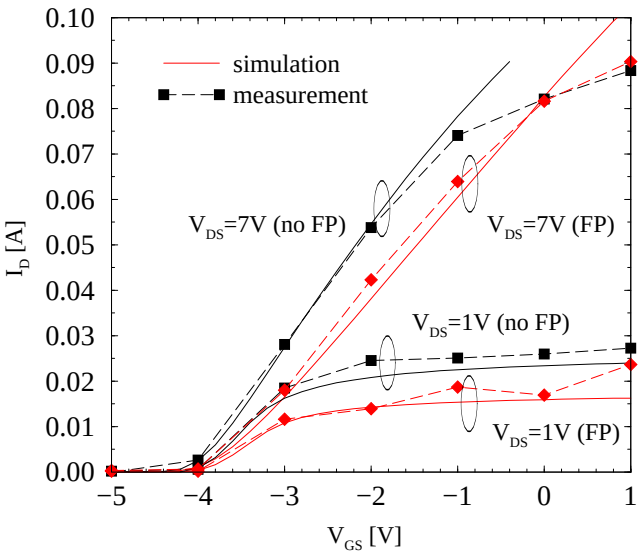

Fig. 5. Comparison of measured (symbols) and simulated (lines) transfer characteristics of HEMTs with and without field plate.

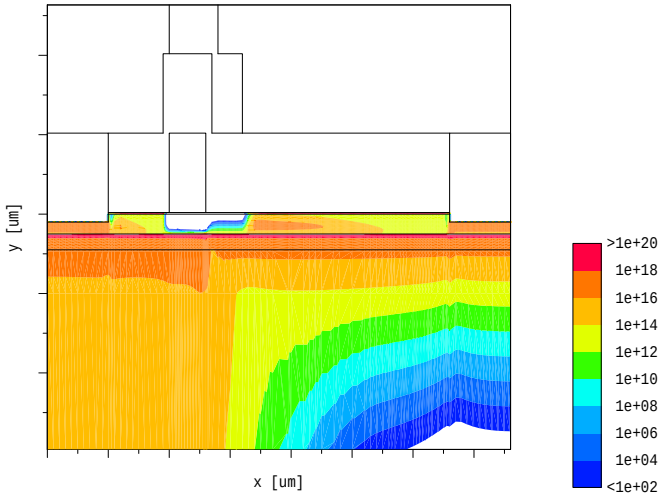

Fig. 4. Simulated electron concentration (given in [cm^{-3}]) in an AlGaN/GaN HEMT with l_g=l_{FP}=600 nm for V_{GS}=0 V and V_{DS}=7 V.

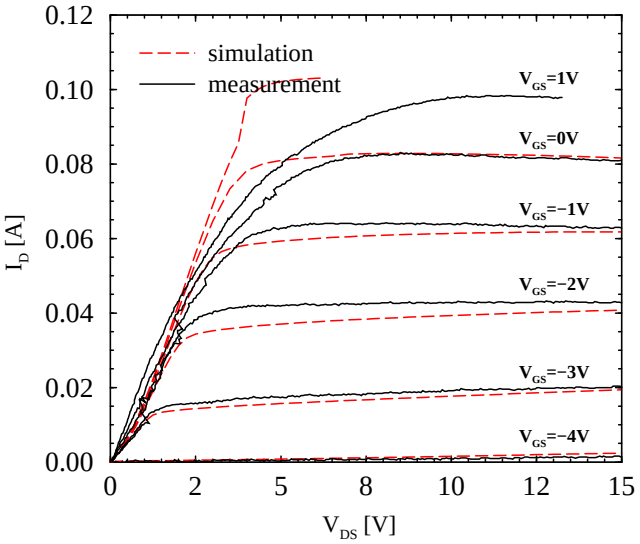

Fig. 6. Output characteristics for 600 nm device with field plate.

IV. Field Plate Optimization

Further we focus on exploring the impact of the field plate. The benefit is an increase of the breakdown voltage and a reduced high-field trapping effect. Overall the power density can be increased significantly [14].

The critical variables associated with the field plate for a given gate length are the field plate length and the SiN thickness (see Fig. 2). While the gate length is crucial for the transit time, the field plate length is the major factor for the size of the electrical field-reshaped region. The nitride thickness controls the onset voltage but has also a significant influence on the maximum electric field.

The difference caused by the field plate is better demonstrated by the electrical field distribution in the channel as shown in Fig. 7. A 50% reduction of the maximum electric field, located at the drain side of the gate edge, is achieved by the introduction of the field plate. A second peak occurs at the field plate edge. We further optimize the critical geometrical values controlling the field distribution.

First we explore the exact distribution for different field plate lengths l_{FP}. Therefore, we simulate devices with 600 nm gate length at V_{GS}=V_{FPS}=-7 V, V_{DS}=60 V. The field plate is varied between 200 nm and 1μm (see Fig. 8). l_{FP}=600 nm appears to be the best choice, since it provides the lowest peak value of the electric field.

Under the same bias conditions we simulate devices with different gate lengths (see Fig. 9). The field plate length is always set equal to the gate length (l_{FP}=l_g). The simulation results show that the optimum field-plate lengths do not scale as much as the gate lengths.

V. Conclusion

A full set of models and model parameters for GaN-based materials has been created based on experimental results and own Monte Carlo simulation data. The analytical models are

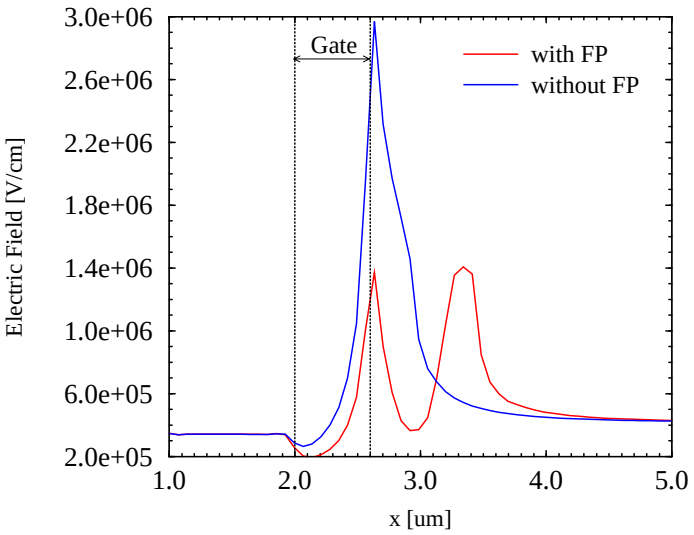

Fig. 7. Simulated electric field along the channel of l_{g}=600 nm HEMTs with and without field plate for V_{GS}=0 V and V_{DS}=7 V.

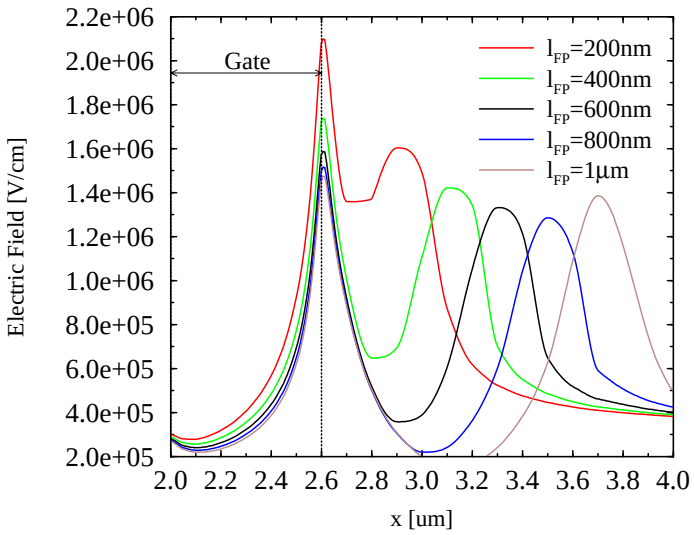

Fig. 8. Simulated electric field along the channel for various field plate lengths l_{FP} (l_{g}=600 nm).

integrated in our two-dimensional device simulator Minimos-NT. The device simulation results show a good agreement with measured electrical data of AlGaN/GaN HEMTs. Such a calibrated tool allows us the consecutive investigation and optimization of the electric field in the channel.

Acknowledgment

Support by the TARGET European Network of Excellence and by the Austrian Science Funds FWF and BMBWK, START Project No.Y247-N13, is acknowledged.

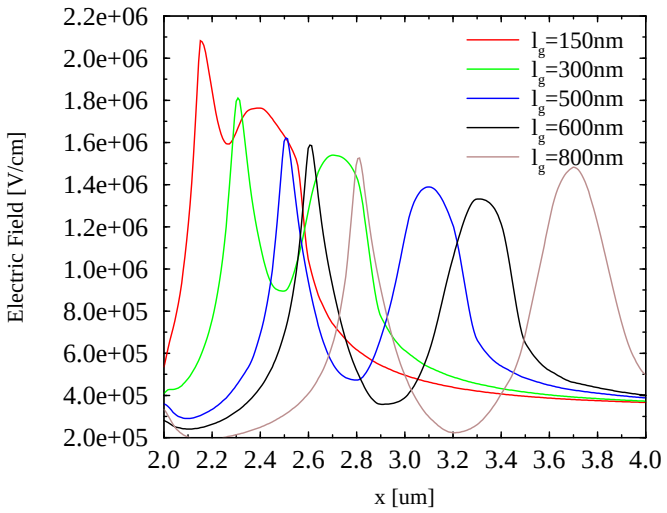

Fig. 9. Simulated electric field along the channel for various gate lengths (l_{FP}=l_{g}).

References

[1] H. Maruska and J. Tietjen, "The Preparation and Properties of Vapor-Deposited Single-Crystal-Line GaN," *Appl. Phys. Lett.*, vol. 15, pp. 327–329, Nov. 1969.

[2] H. Amano, N. Sawaki, I. Akasaki, and Y. Toyoda, "Metalorganic Vapor Phase Epitaxial Growth of a High Quality GaN Film Using an AlN Buffer Layer", *Appl. Phys. Lett.*, vol. 48, pp. 353–355, 1986.

[3] S. Nakamura, N. Iwasa, M. Senoh, and T. Mukai, "Hole Compensation Mechanism of P-Type GaN Films", *J. Appl. Phys.* vol. 31, pp. 1258–1266, 1992.

[4] M. Khan, A. Bhattarai, J. Kuznia, and D. Olson", "High Electron Mobility Transistor Based on a GaN–$Al_xGa_{1-x}N$ Heterojunction", *Appl. Phys. Lett.*, vol. 63, pp. 1214–1215. Aug. 1993.

[5] M. Khan, J. Kuznia, D. Olson, W. Schaff, J. Burm, and M. Shur, "Microwave Performance of a 0.25 μm gate AlGaN/GaN Heterostructure Field Effect Transistor", *Appl. Phys. Lett.*, vol. 65, pp 1121–1123, Aug. 1994.

[6] M. Higashiwaki, T. Matsui, and T. Mimura, "AlGaN/GaN MIS-HFETs with f_T of 163 GHz Using Cat-CVD SiN Gate-Insulating and Passivation Layers", *IEEE Electron Device Lett.*, vol. 27, pp 16–18, Jan. 2006.

[7] N. Zhang, S. Keller, G. Parish, S. Heikman, S. Denbaars, and U. Mishra, "High Breakdown in GaN HEMT with Overlapping Gate Structure", *IEEE Electron Device Lett.*, vol. 21, pp 421–423, Sept. 2000.

[8] F. Conti and M. Conti, "Surface Breakdown in Silicon Planar Diodes Equiped with a Field Plate", *Solid State Electron.*, vol. 15, pp. 93–105, Jan. 1972.

[9] Y. Dora, A. Chakraborty, L. McCarthy, S. Keller, S. DenBaars, and U. Mishra, "High Breakdown Voltage Achieved on AlGaN/GaN HEMTs with Integrated Slant Field Plates", *IEEE Electron Device Lett.*, vol. 27, pp. 713–715, Sept. 2006.

[10] Institute for Microelectronics, Minimos-NT Device and Circuit Simulator, User's Guide, Release 2.0. *http://www.iue.tuwien.ac.at/mmnt*

[11] S. Selberherr, "Analysis and Simulation of Semiconductor Devices", *Springer*, Wien–New York, 1984.

[12] T. Grasser, "Mixed-Mode Device Simulation", Dissertation, Technische Universität Wien, 1999. *http://www.iue.tuwien.ac.at/phd/grasser*

[13] V. Palankovski, A. Marchlewski, E. Ungersböck, and S. Selberherr, "Identification of Transport Parameters for Gallium Nitride Based Semiconductors", *Proc. 5th MATHMOD*, CDROM, Vienna, pp. 14-1–14-9, 2006.

[14] Y. Ando, Y. Okamoto, H. Miyamoto, T. Nakayama, T. Inoue, and M. Kuzuhara, "10-W/mm AlGaN-GaN HFET with a Field Modulating Plate", *IEEE Electron Device Lett.*, vol. 24, pp. 289–291, May 2003.